NEURAL NETWORKS APPROACH FOR PREDICTION OF GAS-LIQUID TWO-PHASE FLOW PATTERN DURING CONVECTIVE CONDENSATION IN MICROSCALE CHANNELS

Araújo D.C., Arcanjo A., Tibiriçá C.B., Nascimento, F.J. and *Ribatski G.
*Author for correspondence
Escola de Engenharia de São Carlos,
University of São Paulo (USP),
São Carlos, 13566-590,
Brazil,
E-mail: ribatski@sc.usp.br

ABSTRACT

In two-phase flow, almost every constitutive relation is flow regime dependent because physical mechanisms that control heat transfer and pressure drop vary with the flow regime. Thus, the identification of flow pattern is an important issue to properly design, and operate two-phase flow systems. In recent years, emphasis has been put on the characteristics of two-phase flow and heat transfer in small and microscale flow passages due to the rapid development of microscale devices, but yet, no general accepted flow-pattern map for microscale channels is available. In this paper, a three-layer, feedforward neural network was designed. Mass velocity, vapor quality and fluid temperature were adopted as input data. The artificial neural network (ANN) was developed based on two-phase flow data for refrigerant R134a in a microscale channel. The validity of the adopted neural network was evaluated by cross validation. The results show that the neural network can provide good flow pattern predictions.

INTRODUCTION

Gas-liquid two-phase flows at both adiabatic and diabatic conditions are very complex physical processes since they combine the characteristics of deformable interface, channel shape, flow direction, and, in some cases, the compressibility of one of the phases [1]. The macroscopic behavior of the flow like pressure drop, wall heat exchanges or mechanical interaction with structures is strongly correlated to the flow regime and can vary from one pattern to another. From an industrial point of view, an optimal exploitation offers durability and safety of the equipment only when the installation operates according to the flow regimes that it was designed for. This means that one has to be able not only to detect instantaneously what the flow pattern is, but also an eventual undesired flow pattern transition must be detected in order to react in the sense of avoiding it, or simply to be aware of it. Thus, it is clear that the use of active control techniques in two-phase flows manipulation and transport systems represents a major technological development in petrochemical or thermonuclear industries among others [2].

NOMENCLATURE

A	[-]	Output variable of ANN
b	[-]	Bias of ANN neuron
d	[mm]	Tube diameter
Er	[-]	Relative Error
G	[kg/m²s]	Mass flux
N	[-]	Neurons in the hidden layer
T_{sat}	[°C]	Saturation Temperature
u	[-]	The net input by adding all the inputs
w	[-]	Weight matrix of ANN connections
x	[-]	Vapor quality
x_i	[-]	ANN input
y	[-]	ANN output

Special character

φ	[-]	Activation Function

Subscripts

c		Numerical data
e		Experimental data
p		Prediction by ANN

It is over 50 years since the first flow pattern map was proposed by Baker [3], who defined flow pattern transitions based upon the superficial gas and liquid velocities for oil and gas flows. Since then, several maps and prediction methods to characterize flow patterns in two-phase flows have been proposed, most of them being based on observations from channels with internal diameters larger than 10mm. Combinations of physical properties with superficial velocities, void fraction and, in the case of diabatic applications, the total mass velocity, and vapor quality have been used to characterize flow pattern transitions in these maps. Some maps for two-

phase flow on tube bundles have also been proposed. Recently, Cheng *et al.* [4] presented a broad review on two-phase flow patterns that is cited here as a comprehensive prospect not only on the historical aspects of flow pattern characterization but also on the actual "status quo" of research that has been performed on this topic [5].

In recent years, emphasis has been put on the characteristics of two-phase flow and heat transfer in small and microscale flow passages due to the rapid development of microscale devices, but yet, no general accepted flow-pattern map for microscale channels is available. This paper focuses on identification of flow pattern in microchannels and aims to provide a neural network for flow pattern prediction of refrigerant R134a.

FLOW PATTERNS IN MICROSCALE CHANNELS

Evaporation in microchannels, often implemented as numerous microchannels in parallel in a cooling element, has seen or is being considered for cooling of computer microprocessors, chemical microreactors, power electronics, automotive air conditioners and other emerging technologies. The typical advantages of a multi-microchannel cooling system are that they are very compact, they can be sandwiched between hot process channels in a stack arrangement, the boiling heat transfer coefficients are very high, very low to very high heat fluxes can be dissipated, fairly uniform temperatures can be produced when required, various materials can be used for their construction and their rapid time response to changes in the thermal cooling load for ease in temperature control [6].

Due to the differences of transport phenomena in microscale channels as compared to conventional size channels or macroscale channels, one very important issue should be clarified about the distinction between microscale and macroscale channels. However, a universal agreement is not clearly established in the literature. Based on engineering practice and application areas such as refrigeration industry in the small tonnage units, compact evaporators employed in automotive, aerospace, air separation, and cryogenic industries, cooling elements in the field of microelectronics, and microelectromechanical systems (MEMS), Kandlikar [7] defined that the distinction between small and conventional size channels is 3 mm [1].

According to Tripplet *et al.* [8] *apud* Thome and Ribastki [6], since the channel diameters for microscale channels are about equal to or smaller than the Laplace length scale, the hydrodynamic interfacial process that are governed by Taylor instability does not apply to capillaries and therefore macrochannel flow pattern transition prediction methods will not work for smaller channels. In microscale channels, the liquid flow is often laminar with typical Reynolds numbers in applications from about 100 to 4000, which is rare in macroscale channels where the opposite is true: the majority of applications have turbulent liquid flow. Based on this, it seems likely that the knowledge developed for macroscale channels under turbulent conditions cannot be directly extended to predict flow pattern transitions in microscale channels. However, it seems that except for stratified flows, the other major flow patterns that are common in large channels also occur in microchannels, although, certain flow pattern details may differs from those in large channels and the boundaries of the various regimes are different.

As observed and characterized by Thome and co-workers [9,10], the flow patterns and their transitions encountered during flow boiling of R-134a in a 0.5mm tube are as follows:

- Bubbly flow: In bubbly flow, the bubbles are smaller in length than the diameter of the tube and the vapor phase is distributed as discrete bubbles in a continuous liquid phase. Figure 1a shows a picture of this regime.
- Bubbly/slug flow: Here both bubbles longer and shorter than the diameter of the channel are observed, as shown in Figure 1b.
- Elongated bubble flow: This regime is characterized by vapor bubbles longer than the diameter of the channel, which are slightly smaller in diameter than the tube. The bubbles are separated from the inner channel wall by a thin film of liquid and from one another by liquid slugs as depicted in Figure 1c.
- Slug/semi-annular flow: Here both slug and semi-annular flows are present. The bubble velocity increases with heat flux and the rear of the elongated bubbles begin to break up (Figure 1d). Coalescence is no longer clean but instead creates a churn-like zone in place of the liquid slug.
- Semi-annular flow: In this flow, liquid slugs are non-existent, as shown in Figure 1e. A liquid film forms at the tube wall with a nearly continuous central vapor core, truncated periodically by churning liquid–vapor zones. It is interesting to emphasize that the churning liquid–vapor zones disappear gradually from the beginning of this regime up to its end.
- Annular flow: In annular flow, a liquid film flows on the tube wall with a continuous central vapor core without churning liquid–vapor zones. There are two types of annular flow, distinctly wavy and relatively smooth, as can be seen in Figure 1f and g, respectively.
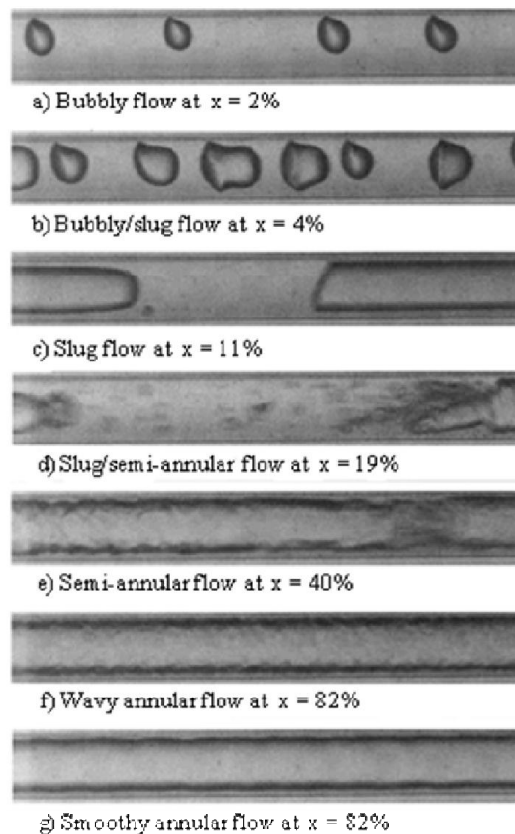
Figure 1 Flow images by Revellin *et al.* [10] for R-134a, d=0.509mm, G=500 kgm^{-2}s^{-1} and T$_{sat}$=30°C at exit of heated channel taken with high-definition, high-speed digital video camera.

FLOW PATTERN PREDICTION METHODS FOR MICROSCALE CHANNELS

To the best of the authors' knowledge, there is no model for flow pattern transition in micro-scale channels [11]. Generally, in the literature concerning micro-scale channels, only curve fitting of dimensionless numbers based on restricted databases studies have been found as, for example, the one by Revellin and Thome [9], among others. Thus, they cannot be considered generalized methods.

Revellin and Thome [9] proposed a flow pattern map for evaporating flows in microchannels for eventual use in mechanistic types of models for flow boiling and two-phase pressure drops. Rather than segregating the observations into the traditional flow regimes and an adiabatic map, the proposed map classifies flows into three types: (i) the *isolated bubble* (IB) regime, where the bubble generation rate is much larger than the bubble coalescence rate and includes both bubbly and slug flows, (ii) the *coalescing bubble* (CB) regime, where the bubble coalescence rate is much larger than the bubble generation rate and exists up to the end of the coalescence process and (iii) the *annular* (A) regime, whose extent is limited by *post dryout* (PD) regime, and begins at the vapor

qualities corresponding to the onset of critical heat flux. The database used was two refrigerants (R-134a and R-245fa) and two channel diameters (0.509mm and 0.790mm). Figure 2 shows an example of the proposed flow pattern in a mass velocity versus vapor quality plot.
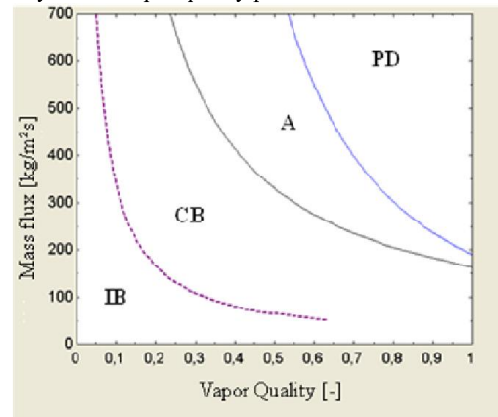

Figure 2 Revellin and Thome [9] map for diabatic flow with R-134a, d=0.5mm and T$_{sat}$=22°C.

Felcar *et al.* [5] developed a flow pattern prediction procedure based on the Taitel and Dukler [12] model for horizontal flows. They incorporated surface tension effects, contact angle and secondary flows on the stratified/annular and intermittent/annular transitions. In order to adjust the empirical coefficients, they used experimental results of air-water flows in microchannels. Figure 3 displays a comparison between the flow pattern predictive method by Felcar *et al.* [5] and some air-water flow pattern data from the literature. Arcanjo *et al.* [13] have compared Felcar et al. [5] predictive method against their experimental results for R134a in a 2.3mm tube and obtained good results, as shown in Figure 4.
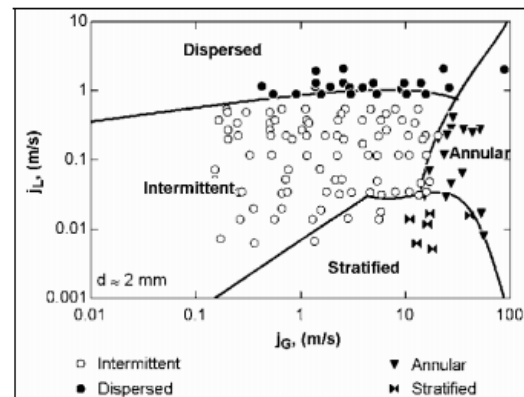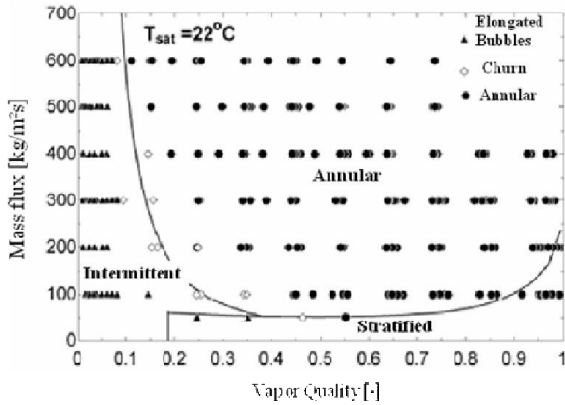

Figure 3 Felcar *et al.* [5] diabatic map

Figure 4　Felcar *et al.* [5] map for diabatic flow with R-134a, d=2.3mm and T_{sat}=22°C [13]

NEURAL NETWORK MODEL FOR THE FLOW PATTERN IDENTIFICATION

Neural networks, an analytical tool imitating the neural aspect of the human brain, are excellent at pattern recognition and trend prediction for processes that are nonlinear, poorly understood and too complex for accurate mathematical modeling [14, 15]. They seem good predictive tools to be applied to multiphase flow systems, and when properly designed and trained, can potentially improve on-line monitoring and diagnostics [16].

An artificial neural network (ANN) consists of a great number of interconnected neurons. A block diagram of the model of a neuron is shown in Figure 5. A neuron is a basic information processing and operating unit in a neural network. Specifically, a signal x_i is input to connect to a neuron with the synaptic weight w_i, and then all input signals weighted by their respective synapses are summed as a net input u. A bias b is applied to the neuron so that the increase or decrease of net input depends on whether the bias is positive or negative. Finally the increased or decreased net input is imported into an activation function resulting in the output. The activation function is so developed that the amplitude of the net output of a neuron is limited. The input-to-output operation of a neuron is formulized mathematically as follows:

$$u^k = \sum_{i=1}^{m} w_i^k x_i \qquad (1)$$

$$y^k = \varphi\left(u^k + b^k\right) = \varphi\left(\sum_{i=1}^{m} w_i^k x_i + b^k\right) = \varphi\left(\sum_{i=1}^{m} w_i^k x_i\right) \qquad (2)$$

It is noted that the bias may be accounted for as a new input fixed at $x_o = \pm 1$ with its weight b and then combined with the original inputs as a whole input. Therefore the above equation has been reformulated to combine inputs and bias by replacing subscript 1 with 0 as seen in the last term of the right-hand side of equation (2) [17].
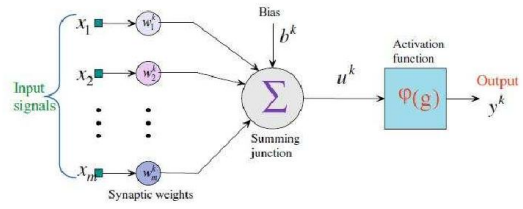

Figure 5　Nonlinear model of a neuron [17]

Recently, some successful applications of neural networks to multiphase flow problems have demonstrated their enormous potential. Abro *et al.* [18] determined the void fraction and flow regime of oil/gas flow using a neural network trained by simulated data based on gamma-ray densitometry. Mi *et al.* [19] applied a neural network for the two-phase flow pattern recognition in a vertical channel using signals from electric capacitance probes. Xie *et al.* [20] designed an artificial neural network for the classification of flow patterns in three-phase systems using pressure signals. The above findings have shown that neural networks are capable of learning to recognize flow patterns based on pressure fluctuation and some other flow-induced signals [16].

Experimental Data and ANN Structure

The tests were run for R134a evaporating in a stainless steel tube with diameter of 2.32 mm, mass velocities from 50 to 600 kg/m²s and saturation temperatures of 22°C, 31°C and 41°C. The tube was heated by applying a direct DC current to its surface. Images from a high-speed video-camera (8000 frames/s) obtained through a transparent tube just downstream of the heated section were used to identify the following flow patterns: bubbly, elongated bubbles, churn and annular. Dryout conditions were also characterized.

Among the various kinds of ANNs that exist, the feedforward configuration has become the most popular in engineering applications [21]. A multilayer perception is a feedforward ANN model that has one input layer, at least one hidden layer and one output layer. Figure 6 shows the network structure for this problem, where N represents the number of neurons of the hidden layer, x_1 represents the mass flux, x_2 the saturation temperature and x_3 the vapor quality.
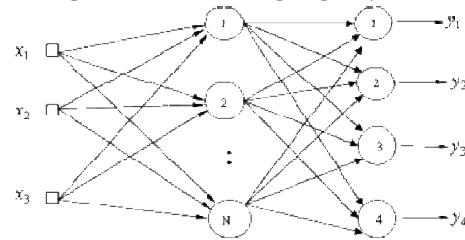

Figure 6　ANN Structure

The output standardization, representing the flow pattern, was defined as follows in Table 1.

Flow Pattern	y_1	y_2	y_3	y_4
Annular	1	0	0	0
Churn	0	1	0	0
Slug	0	0	1	0
Bubbles	0	0	0	1

Table 1   Output standardization

ANN Training and Assessment

As shown in Figure 6, a three-neuron-layer network was designed. The neurons in the input layer had a piecewise linear activation function, while the neurons in the hidden and the output layers used the logistic activation function. The back-propagation learning algorithm was used. The learning rate was set to 0.1 and the relative error of every predicted output was defined by

$$Er = \frac{|A^e - A^p|}{A^e} \qquad (3)$$

where A^p is the predicted results, that is output of ANN, A^e is the experimental data, that is the target output. The maximum Er was set to 10^{-6}.

A total of 759 groups of normalized mass flux, vapor quality and saturation temperature data were available for the neural networks. Following common practice, a fraction of the obtained data (80%, or 607 data records) was selected for training the neural networks, which constituted the so-called 'calibration data', and the other data records were used to validate the network.

The number of the layers, input neuron and output neuron was fixed and the determination of the number of neurons in the hidden layer was carried out with cross-validation. There were tested ANNs with 5, 10, 20, 30, 40 and 50 neurons in the hidden layer. Table 2 shows the tested topologies and their respective errors. By consideration of the ANN performance, we choose the topology with 10 neurons in the hidden layer.

Topology	Error
5 neurons	3,29%
10 neurons	2,63%
15 neurons	3,29%
20 neurons	3,29%
30 neurons	3,29%
40 neurons	5,26%
50 neurons	overfiting

Table 2   Topology errors

DISCUSSION

Figure 7 shows the flow map created by the ANN. Figure 8 and Figure 9 showa comparison of the map created against the flow pattern transitions provided by the method of

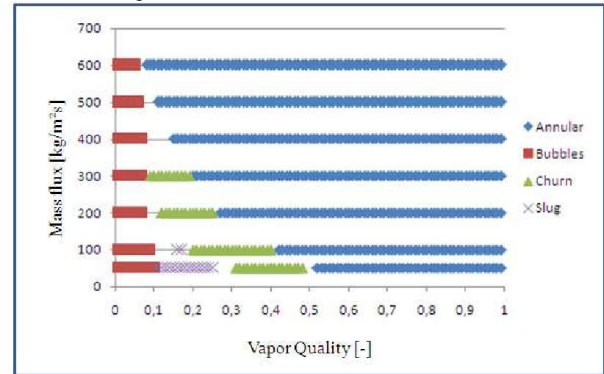Revellin and Thome [9] and Felcar *et al.* [5] , respectively, for saturation temperatures of 22°C.

Figure 7   ANN Map for R-134a, d=2.3mm and T_{sat}=22ºC
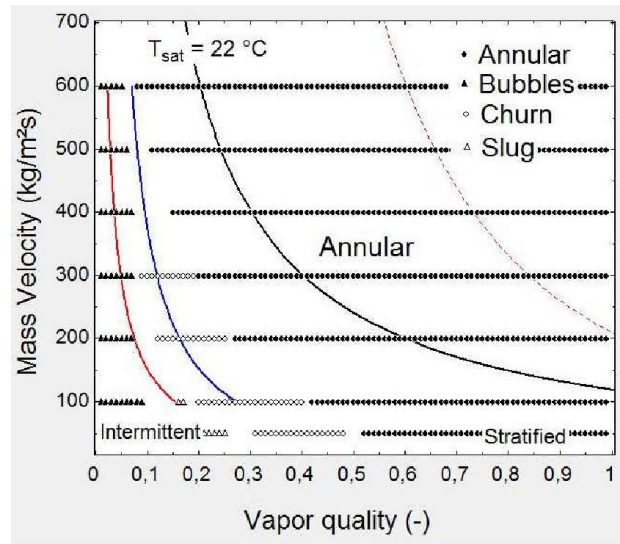

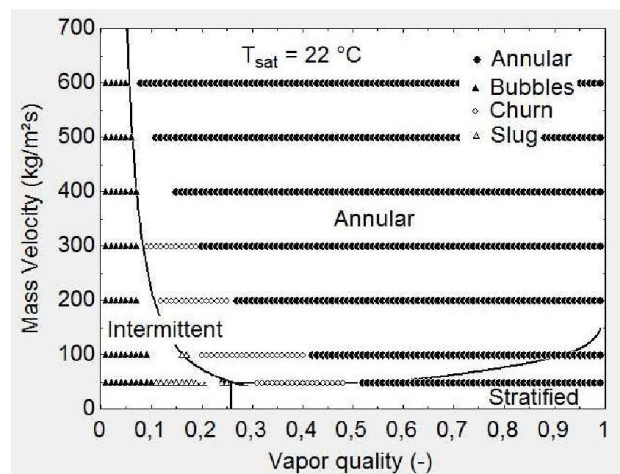**Figure 8**   Revellin and Thome [9] map for ANN database

Figure 9   Felcar *et al.* [5] map for ANN database

As can be observed, Revellin and Thome [9] method failed into predict the present database. A transition to stratified flows is not provided by this method, since was based only on data for tube diameters smaller than 1mm, a condition for which stratified flows are not feasible [13].

In general, Felcar *et al.* [5] method predicts relatively well the database obtained with the ANN. The transition from intermittent to annular is predicted relatively well, capturing the annular-intermittent vapor quality threshold decreases with increasing mass velocity.

CONCLUSION

In the present study it was applied the ANN approach to accurately model the flow patterns of the refrigerant R134a in a microscale channel. A summary of the conclusions drawn from the results of the present investigation is as follows:

a) Because of the inherent attributes of the ANN technique, ANNs can predict experimental data with errors of the same order as the uncertainty of the measurements. It can be said that the multilayer perceptron ANN is a good method for flow pattern predictions, since the flow pattern map created shown good concordance with an existing method.

b) In general, the flow pattern predictive method proposed by Felcar *et al.* [5] agrees quite well with the database created by the ANN. However, this method should be further improved in order to more accurately predict the flow pattern transitions at low mass velocities and high vapor qualities. It should be also mentioned that stratified flows seem improbable for flow boiling of R134a in a 2.32mm diameter tube.

ACKNOWLEDGEMENTS

REFERENCES

[1] Cheng L., Ribatski, G., and Thome, J.R., Two-phase flow patterns and flow-pattern maps: fundamentals and applications, *Applied Mechanics Reviews,* Vol. 61, No. 5, July 2008, p. 050802-1.

[2] Hervieu, E., and Seleghim Jr., P., An objective indicator for two-phase flow pattern transition, *Nuclear Engineering and Design,* Vol. 184, No. 2-3, April 1998, pp. 421-435.

[3] Baker, O., Simultaneous Flow of Oil and Gas, *Oil and Gas Journal*, Vol. 53, No. 6, July 1954, pp. 185-195.

[4] Cheng, L., Ribatski, G., Wojtan, L., and Thome, J.R., Erratum to: New flow boiling heat transfer model and flow pattern map for carbon dioxid evaporating inside tubes, [*Heat Mass Transfer*, Vol. 49, No. 21-22, 2006, pp. 4082-4094] *International Journal of Heat and Mass Transfer*, Vol. 50, No. 1-2, January 2007, p. 391.

[5] Felcar, H.O.M., Ribatski, G., and Jabardo, J.M.S., A gas-liquid flow pattern predictive method for macro and mini-scale round channels, *Proceedings of the 10th UK Nacional Heat Transfer Conference*, Edinburgh, Scotland, UK, September 2007.

[6] Thome, J.R., and Ribatski, G., Boiling and two-phase flow in microchannels, *Handbook of Micro Reactors Vol.1: Fundamentals, Operations and Catalysts*, 2009.

[7] Kandlikar, S.G., Fundamental Issues Related to Flow Boiling in Minichannels and Microchannels, *Experimental Thermal and Fluid Science*, Vol. 26, No. 2-4, June 2002, pp. 389–407.

[8] Triplett K.A., Ghiaasiaan S.M., Abdel-Kahalik S.I., and. Sadowski D.L., Gas–liquid two-phase flow in microchannels, Part I: two-phase flow patterns, *International Journal of Multiphase Flow*, Vol. 25, No. 3, April 1999, pp. 377–394.

[9] Revellin R., and Thome J.R., A new type of diabatic flow pattern map for boiling heat transfer in microchannels, *Journal Micromechanics and Microengineering*, Vol. 17, No. 4, April 2007, pp. 788–796.

[10] Revellin R., Dupont V., Ursenbacher T., Thome J.R., and Zun I., Characterization of diabatic two-phase flows in microchannels: flow parameter results for R-134a in a 0.5 mm channel, *International Journal of Multiphase Flow*, Vol. 32, No. 7, July 2006, pp. 755–774.

[11] Tibiriçá, C.B., Felcar, H.O.M., and Ribatski, G. An analysis of experimental data and prediction methods for critical heat fluxes in micro-scale channels. *In: 5th European Thermal-Sciences Conference*, Eindhoven, the Netherlands, 18-22 May 2008.

[12] Taitel Y., and Dukler, A.E., A model for predicting regime transitions in horizontal and near horizontal gas-liquid flow, *AIChE Journal*, Vol. 22, No. 1, January 1976, pp. 47-55.

[13] Arcanjo A.A., Freitas, J.O., Tibiriçá, C.B., and Ribatski, G., Two-phase flow characteristics during flow boiling of halocarbon refrigerants in microscale channels, *in: ECI International Conference on Boiling Heat Transfer*, Florianópolis, SC, Brazil, 3-7 May 2009.

[14] Wills M.J., Montague G.A., and Massimo C.D., Artificial neural networks in process estimation and control, *Automatica*, Vol. 28, No. 6, November 1992, pp.1181–1187.

[15] Armitage A.F., Neural networks in measurement and control, *Measurement and Control*, Vol. 28, No. 7, 1995, pp. 208–215.

[16] Sun, Z., Zhang, H., Neural networks approach for prediction of gas–liquid two-phase flow pattern based on frequency domain analysis of vortex flowmeter signals, *Measurement Science and Technology*, Vol. 19, No. 1, January 2008, p. 15401.

[17] Xie G., Sunden B., Wang Q., and Tang L., Performance predictions of laminar and turbulent heat transfer and fluid flow of heat exchangers having large tube-diameter and large tube-row by artificial neural networks, *International Journal of Heat and Mass Transfer*, Vol. 52, No. 11-12, March 2009, pp. 2484-2497.

[18] Abro E., Khoryakov V.A., Johansen G.A., and Kocbach L., Determination of void fraction and flow regime using a neural network trained on simulated data based on gamma-ray densitometry, *Measurement Science and Technology,* Vol. 10, No. 7, July 1999, pp. 619–30.

[19] Mi Y., Ishii M., and Tsoukalas L.H., Flow regime identification methodology with neural networks and two-phase models, *Nuclear Engineering and Design*, Vol. 204, No. 1-3, February 2001, pp. 87–100.

[20] Xie T., Ghiaasiaan S.M., and Karrila S., Artificial neural network approach for flow regime classification in gas–liquid-fiber flows based on frequency domain analysis of pressure signals, *Chemical Engineering Science*, Vol. 59, No. 11, June 2004, pp. 2241–2251.

[21] Pacheco-Vega A., Sen M., Yang K.T., and McClain R.L., Neural network analysis of fin-tube refrigerating heat exchanger with limited experimental data, *International Journal of Heat and Mass Transfer*, Vol. 44, No. 4, February 2001, pp. 763-770.